JOURNAL OF MATERIALS SCIENCE **34** (1999) 579–585

Indentation fatigue testing of soda-lime silicate glass

V. M. SGLAVO*
Dipartimento di Ingegneria dei Materiali, Università di Trento, Via Mesiano 77, 38050 Trento (Italy)
E-mail: sglavo@ing.unitn.it

D. J. GREEN
Department of Materials Science and Engineering, The Pennsylvania State University, University Park, PA 16802 (USA)

Dynamic, cyclic and static fatigue testing was performed on soda lime silicate glass using indentation strength measurements. Using the conventional analysis, the cyclic and static fatigue data were inconsistent with the remaining data for the case when the indentations were annealed prior to testing. Using an analysis that included the measured variations in the fracture mechanics geometric parameters, all three data sets were consistent. Using a numerical analysis, the lifetime for materials in the static and cyclic fatigue tests was shown to be sensitive to variations in the stress intensity factor at short crack lengths. It is therefore very important to understand any crack size dependence of the fracture mechanics parameters in this crack size region for accurate lifetime predictions.

1. Introduction

The use of glass in many structural application is sometimes limited by the phenomenon known as fatigue. This term is used to indicate a particular behaviour of this class of material corresponding to a sub-critical propagation of defects which occur when the specimen is subjected to a load in a corrosive environment. What makes this phenomenon particularly important is that for most glasses the corrosive environment can simply be the moisture in the atmosphere [1–3].

Great effort has been devoted to the analysis of such behaviour in glass and especially in soda-lime silicate glasses. Different techniques based on typical fracture mechanics tests have been used to measure the crack propagation velocity as a function of the applied load and of the environment. On the basis of these tests, fatigue behaviour is usually described through the empirical relation [4]:

$$v = v_0 \left(\frac{K}{K_c} \right)^n \tag{1}$$

where v is the crack velocity, K the applied stress intensity factor, K_c the fracture toughness while v_0 and n are two parameters that depend on the material and the environment.

Indentation techniques represent a powerful tool for the analysis of the fatigue behaviour of glass. Surface cracks can be easily produced by Vickers indentation. These artificial defects represent well the behaviour of inherent flaws with the advantage of being reproducible and large enough to be observed by an optical microscope. The sub-critical propagation of indentation cracks in soda-lime silicate glass during the indentation test was studied in detail by Sglavo and Green [5]. Other authors [6–9] observed the propagation of the radial cracks after the indentation under the sole influence of the residual stress field produced by the impression. These methods allowed the fatigue behaviour of glass to be analyzed and, in some cases, the fatigue limit could be evaluated [10, 11]. The sub-critical growth of indentation cracks under the effect of an external load has been studied extensively both in static and dynamic fatigue [3, 12–23]. In these tests the use of controlled flaws allowed the typical problem connected to the strength measurement in glasses, that is the high dispersion of the experimental strength data, to be avoided. Detailed procedures have been presented in the past for the measurement of v_0 and n by dynamic fatigue tests on indented specimens [13, 24]. Although there have been extensive studies in the fatigue behavior of glass, there are still outstanding problems. For example, in some previous papers [21], discrepancies were observed between theoretical calculations and experimental measurements in static fatigue tests on indented specimens in which the residual stress field was removed by an annealing process. It was shown that only if a crack shape factor varied with crack size could these disagreements be eliminated. Conversely, the proposed theory was shown to work quite well for as-indented samples [21].

* Corresponding author. Tel. +39-461-882468; fax +39-461-881977; e-mail: sglavo@ing.unitn.it.

In this paper experimental data obtained from fatigue tests under dynamic, static and cyclic conditions are compared to predictions calculated using the crack shape factor results presented in a previous paper. A detailed comparison among different loading conditions is performed in order to point out the effect of the annealing condition and the crack shape factor variability on the theoretical predictions.

2. Experimental procedure

Commercial soda-lime-silica glass sheets were used in this work. The composition of the glass was (wt %): 71 SiO_2, 13 Na_2O, 1 Al_2O_3, 10 CaO, 1 MgO, 1 other. Bars (nominally $2\times5\times50\,mm^3$) were obtained from the sheets using a diamond saw. The edges were polished with diamond paste in order to remove large defects created during the cutting procedure. The samples were then annealed at 540 °C for 24 h. A cooling rate of approximately 1 °C/min was used.

Vickers indentation tests were conducted in laboratory air (relative humidity ≈45%; temperature ≈25 °C) using a load of 9.8 N. The indenter was at the maximum load for ≈15 s. The indented bars were then stored in deionized water for 48 h prior to testing in order to allow the cracks to grow sub-critically into a "stabilized" configuration [21]. A certain fraction of the specimens were annealed in air using the same procedure described previously.

Mechanical tests were performed using a four-point bending configuration with inner and outer spans equal to 20 mm and 40 mm, respectively. Both as-indented and annealed specimens were subjected to mechanical tests. Dynamic, static and cyclic fatigue tests were performed in deionized water. Cross-head speeds ranging from 1 μm/min to 10 mm/min were used in the dynamic fatigue tests. Five bars were tested at each stressing rate. Static fatigue tests were performed using constant loads ranging from 21 MPa to 35 MPa for as-indented specimens and from 32 MPa to 44 MPa for annealed specimens. These stress levels guaranteed the measurement of lifetimes between ≈20 s and ≈7 h. Cyclic fatigue tests were performed using a loading ratio $R=\sigma_{min}/\sigma_{max}$ (σ_{min} = minimum applied stress, σ_{max} = maximum applied stress) equal to zero. In this way, indentation cracks were subjected to a tensile stress variable with time, t, as:

$$\sigma = \frac{1}{2}\sigma_{max}(1-\cos(2\pi f t)) \tag{2}$$

where the frequency, f, was fixed to 1 Hz for all tests. The maximum stress was varied from 25 MPa to 40 MPa for as-indented bars and from 35 MPa to 45 MPa for annealed samples. Some strength test were performed in silicon oil to characterize the behavior of the glass in an inert environment [21].

3. Results and discussion

The results of dynamic fatigue tests are shown in Fig. 1. Strength, σ_f, measured in the water environment increases with increasing stressing rate, $\dot{\sigma}$, for both as-indented and annealed specimens. Data are included in the figure to show the inert strength levels, which are higher than the dynamic strength even at the highest stressing rate. This demonstrates the important effect of stress corrosion even in tests with duration less than 1 s.

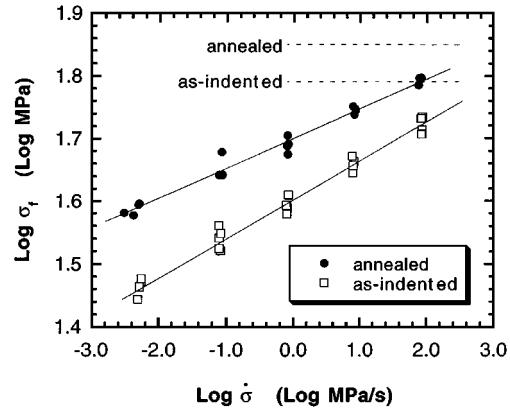

Figure 1 Dynamic fatigue plot for as-indented and annealed specimens. Dashed lines represent the strength measured in the inert environment. Fitted lines are calculated according to Equations 3 and 4 for as-indented and annealed samples, respectively.

Data shown in Fig. 1 were used for the determination of fatigue parameters n and v_0. It has been shown in previous papers [24, 25] that the strength of as-indented specimens, under conditions of dynamic fatigue, can be espressed as:

$$\sigma_f = \zeta\dot{\sigma}^{1/(n'+1)} \tag{3}$$

where

$$\zeta = \left(\frac{2.84n'^{0.462}\sigma_i^{n'}c_m}{v_0}\right)^{1/n'+1}, \tag{3a}$$

$$n' = 0.763n, \tag{3b}$$

c_m represents the critical radial crack length and σ_i is the strength in the inert environment. In order to measure c_m the following steps were followed. Three indentations were produced in the middle region of approximately 10 bars following the same procedure previously described. These indented samples were then broken in silicone oil. The two indentations on each specimen which did not fail upon bending were manually broken and the fracture surfaces were observed by an optical microscope. In this way, the crack shape evolution upon loading up to critical condition could be determined [21]. The values of c_m and σ_i are shown in Table I.

When the residual stress field generated during the indentation is removed by annealing, the strength as a function of the stressing rate can be expressed as [4]:

$$\sigma_f = \zeta\dot{\sigma}^{1/(n+1)} \tag{4}$$

where

$$\zeta = \left(\frac{2(n+1)\sigma_i^n c_0}{(n-2)v_0}\right)^{1/n+1} \tag{4b}$$

TABLE I Initial crack length, c_0, crack length at instability, c_m, and inert strength, σ_i, for as-indented and annealed specimens

	c_0 (μm)	c_m (μm)	σ_i (MPa)
as-indented	120 ± 4	152 ± 11	61.6 ± 1.5
annealed	121 ± 3	138 ± 8	71.3 ± 2.2

TABLE II Fatigue parameter for as-indented and annealed specimens calculated from dynamic fatigue tests

	n	v_0 (mm/s)
as-indented	20.1 ± 0.7	28.8 ± 6.4
annealed	19.9 ± 0.7	6.4 ± 1.4

c_0 being the initial crack length, which can be measured directly on the indentation site (Table I).

It must be pointed out that Equations 3 and 4 are evaluated on the basis of Equation 1 and assuming the following relation for the stress intensity factor [3, 21]:

$$K = \chi P/c^{1.5} + \psi\sigma c^{0.5} \tag{5}$$

where P is the indentation load, c the radial crack length, ψ the crack shape factor and χ the residual stress factor ($\chi = 0$ for annealed specimens). The latter two factors are considered as constant in deriving Equations 3 and 4 [24, 25].

The linear interpolation of $\log \sigma_f$ against $\log \dot{\sigma}$ (Fig. 1) allows the calculation of n and v_0 on the basis of Equations 3 and 4. Calculated values for n and v_0 are shown in Table II. Values calculated for as-indented and annealed specimens are consistent within data scatter. In addition, these values agree with data reported in the literature for soda-lime silicate glass [12, 13, 21, 26]. These results confirm the validity of the measurement of n and v_0 by dynamic fatigue tests both on as-indented and on annealed specimens. For as-indented specimens the strength has to be measured both in the active environment for different stressing rates and in an inert environment. The crack length at instability also has to be determined. For annealed specimens, initial crack length must be measured and the strength has to be determined in the corrosive and in the inert ambient. Nevertheless, the residual stress associated with indentation needs to be completely removed before testing. The great advantage of the dynamic fatigue technique lies in the limited scatter of the strength values, which allows precise determination of the fatigue parameters. It is clear, therefore, that the ease of testing makes this technique preferable to tests in which fracture mechanics samples containing large cracks have to be used.

Fig. 2 shows the results of the static fatigue tests. As expected, lifetimes for annealed specimens are larger than for as-indented samples due to the removal of the indentation residual stress field.

Theoretical predictions are included in Fig. 2 together with experimental data. Lifetime predictions for static fatigue tests (Fig. 2) were calculated on the basis of the fatigue parameters calculated by dynamic fatigue tests. Both (n; v_0) couples determined previously were used, but no appreciable differences could be detected. Therefore, only data obtained using fatigue parameters calculated from as-indented specimens will be shown. The time-to-failure in static fatigue testing can be generally calculated by solving the integral [4, 21]:

$$T_f = \frac{K_c^n}{v_0} \int_{c_0}^{c_f} \frac{1}{(\sigma\psi c^{0.5} + \chi P c^{-1.5})}\, dc \tag{6}$$

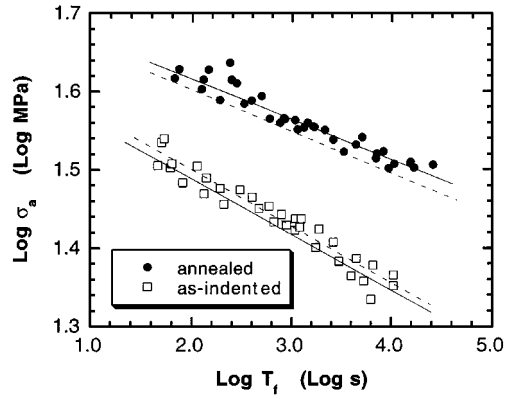

Figure 2 Static fatigue plot for as-indented and annealed specimens. Dashed and solid lines represent the theoretical lifetime predictions calculated by using constant and variable ψ and χ values, respectively, in Equation 6.

where, c_f is the crack length at failure which satisfies the equation:

$$\sigma\psi c_f^{0.5} + \chi P c_f^{-1.5} = K_c \tag{6a}$$

As pointed out earlier, the crack shape and residual stress factors are usually considered as constant during crack propagation. In this case, they can be calculated from the strength and the crack length at instability measured under inert conditions. For as-indented specimens, if ψ and χ are constant, one can demonstrate that [27, 28]:

$$\psi = \frac{3K_c}{4\sigma_m c_i^{0.5}} \tag{7}$$

and

$$\chi = \frac{c_m^{1.5} K_c}{4P} \tag{8}$$

Values equal to 0.71 and 0.034 were calculated from the data reported in Table I using Equations (7) and (8) for ψ and χ, respectively, assuming $K_c = 0.72$ MPa $\sqrt{\text{m}}$. For annealed specimens, χ is zero and the crack shape factor can be calculated as:

$$\psi = \frac{K_c}{\sigma_i c_m^{0.5}} \tag{9}$$

A value equal to $\psi = 0.86$ was calculated for the annealed samples.

The integral in Equation (6) was solved using the calculated ψ and χ values. Lifetime predictions are shown in Fig. 2. The agreement between predictions and experimental data is good only for the as-indented specimens. For annealed samples, the predictions underestimate the time-to-failure for each stress level. Similar results were obtained also in a previous work on a similar soda-lime silicate glass [21].

Cyclic fatigue tests furnished results similar to those obtained in static fatigue. Fig. 3 shows experimental data in terms of number of cycles to failure, N_f, as a function of the maximum stress. Theoretical predictions are also included. These were obtained by

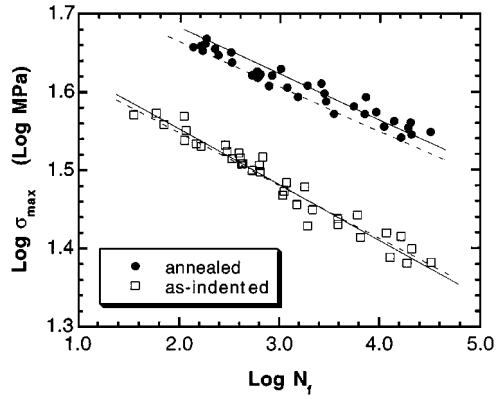

Figure 3 Cyclic fatigue plot of the number of cycles-to-failure, N_f, as a function of the maximum stress, σ_{max}, for as-indented and annealed specimens. Dashed and solid lines represent the theoretical lifetime predictions calculated by using constant and variable ψ and χ values, respectively, in Equation 6.

inserting the expression for σ in cyclic fatigue (Equation 2) in Equation 6 and by the numerical resolution of the obtained integral. It is clear that, since $f = 1$ Hz, N_f coincides with the time-to-failure expressed in seconds. If the constant values of ψ and χ previously calculated are used, predictions are in agreement with experimental data only for as-indented specimens (Fig. 3). Lifetime for annealed specimens is therefore underestimated also in cyclic fatigue.

In a previous paper [29], Sglavo and Green showed that crack shape and residual stress factors are not constant during the propagation of indentation cracks in soda-lime silicate glass. Values of ψ and χ were experimentally measured as function of the crack size and the trends are shown in Fig. 4 [29]. These variable values for ψ and χ are used for theoretical lifetime calculations both in static and in cyclic fatigue. Numerical procedures easily allow considering the variability in ψ and χ for increasing crack length in the relation of Equation 6. The results are shown in Figs 2 and 3. A good agreement between experimental and theoretical data is obtained both for as-indented and for annealed specimens.

The theoretical predictions obtained for the cyclic fatigue tests indicate that similar mechanisms must be controlling both static and cyclic fatigue in soda-lime-silica glass, at least when tensile loads are applied. This implies that no additional terms have to be included in

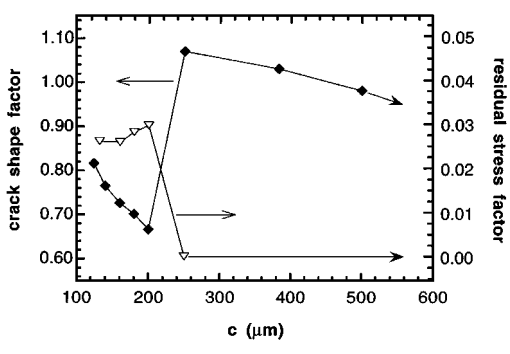

Figure 4 Crack shape and residual stress factor as function of the crack length. From [29].

the definition of the crack propagation function when alternating stresses are present, as in some ceramic materials [30–33].

At this point it is clear that the application of normal indentation fracture mechanics principles leads to different results in dynamic, static and cyclic fatigue. Crack shape and residual stress factors can be considered as constant in the analysis of dynamic fatigue test results. Conversely, in static and dynamic fatigue tests theoretical predictions agree with experimental data only if variable ψ and χ values are included in the analysis. The aim of the next section is to analyse in detail the effect of ψ and χ variability on sub-critical crack propagation with regard to the way the load is applied as a function of time.

4. Numerical analysis

The sub-critical propagation of indentation radial cracks was simulated numerically both in as-indented and annealed specimens. The crack length, c, as a function of time, t, was evaluated by the numerical resolution of the differential equation:

$$\frac{dc}{dt} = \frac{v_0}{K_c^n}(\psi(c)\sigma(t)c^{0.5} + \chi(c)Pc^{1.5})^n \qquad (10)$$

which can be directly obtained from Equation 1. At each time increment the crack length is therefore uniquely defined, and stress intensity factor can be calculated through Equation 5. Failure is recorded when the condition defined in Equation 6a is fulfilled. For the resolution of Equation 10 the fatigue parameters measured by dynamic fatigue tests on as-indented specimens (Table II) were used and the initial crack length, c_0, reported in Table I was considered as the boundary condition. In order to analyse the influence of ψ and χ variability as function of c the resolution of Equation 10 was performed using either constant values previously calculated (condition A) or the data reported in [29] (condition B).

Fig. 5 shows the stress intensity factor as a function of crack length for as-indented and annealed specimens in static fatigue test. In as-indented specimens, K is initially a decreasing function showing similar trends for the two conditions. Then, for crack lengths larger than $\approx$200 μm, the stress intensity factor increases up to failure. The increase is more rapid under condition B than A. Conversely, in annealed samples, K is always an increasing function of the crack length but in this case the increase is more rapid under condition A when the crack size is small. For $c \approx 200$ μm the stress intensity factor shows a sharp increase under condition B, which implies larger K values in condition B than in A.

The features pointed out in K vs c trends are of fundamental importance in understanding the differences in the behaviour between as-indented and annealed specimens under conditions A or B. The value of the stress intensity factor defines the crack velocity at each instant and, therefore, is intimately related to the lifetime of the material.

Crack propagation can be simulated in static fatigue on the basis of the data presented in Fig. 5. Fig. 6 shows

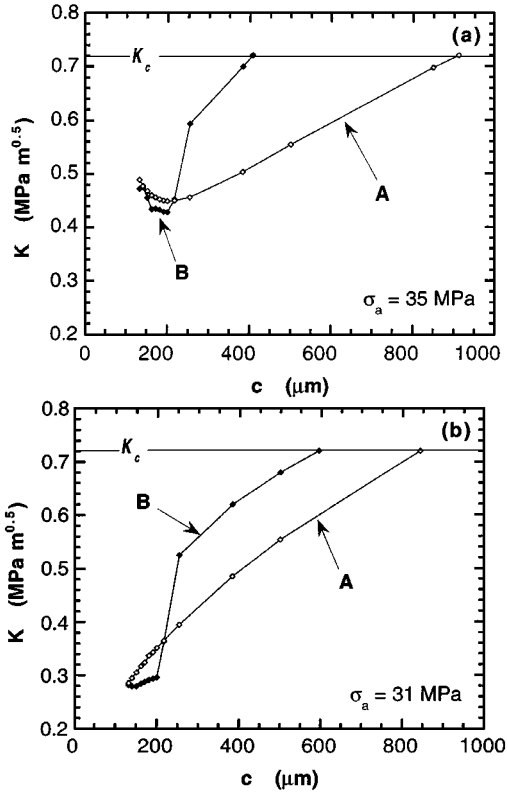

Figure 5 Stress intensity factor as a function of the crack length for as-indented (a) and annealed (b) specimens in the static fatigue test. The stress intensity factor was evaluated according to Equation 5 under the condition of constant (condition A) and variable (condition B) ψ and χ values. The constant applied stress and the critical stress intensity factor [21] level are shown.

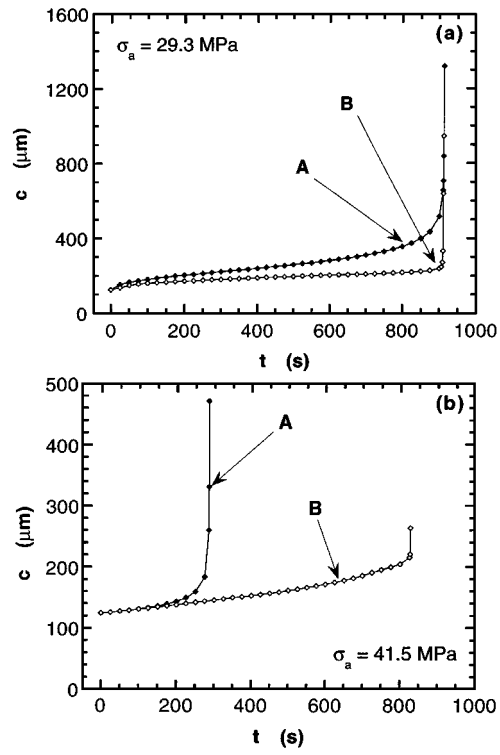

Figure 6 Evolution of the crack size as a function of time for as-indented (a) and annealed (b) specimens in the static fatigue test. Crack length was evaluated as a function of time by the resolution of Equation 10 under the condition of constant (condition A) and variable (condition B) ψ and χ values. The constant applied stress is shown.

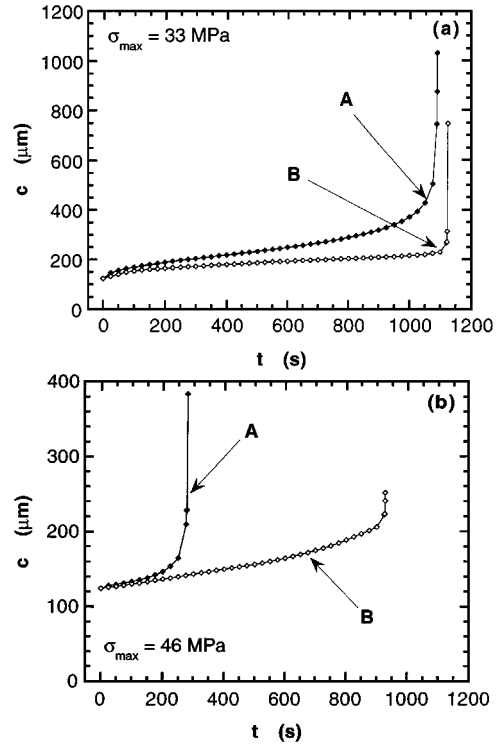

Figure 7 Evolution of the crack size as a function of time for for as-indented (a) and annealed (b) specimens in the cyclic fatigue test. Crack length was evaluated as a function of time by the resolution of Equation 10 under the condition of constant (condition A) and variable (condition B) ψ and χ values. The maximum applied stress is shown.

the crack size as a function of time for as-indented and annealed specimens subjected to a constant load. Similar results were obtained regardless of the applied stress level. For as-indented samples, the time-to-failure is the same under both conditions A and B. A different result is obtained for annealed specimens where the lifetime is noticeably shorter when the crack shape factor is considered to be constant. This result is in agreement with experimental data shown in Fig. 2.

Similar behaviour was obtained in the simulation of cyclic fatigue tests performed using a loading ratio equal to zero. The results are shown in Fig. 7. For as-indented samples the time-to-failure, and therefore N_f, is invariant moving from condition A to B. Conversely, large differences are observed for annealed specimens as was observed in the experimental results.

The predictions calculated for static and cyclic fatigue can be discussed on the basis of data shown in Figs 4 and 5. For annealed specimens distinct differences in the K vs c trend are detected between conditions A and B. This is the result of ψ being a decreasing function of crack size in the first stages of propagation. In fact, for annealed samples, $K = \psi\sigma\sqrt{c}$ and when c is small the stress intensity factor is small, even more so if ψ is a decreasing function of crack length. This effect is then amplified by the effect on crack velocity, which is proportional to K^n where n has a value as large as 20. The first stage of crack propagation (up to $\approx$200 μm) can be considered as the rate limiting step, and the values assumed by ψ are crucial in defining the overall time-to-failure. The influence of ψ as a decreasing function of c is evident

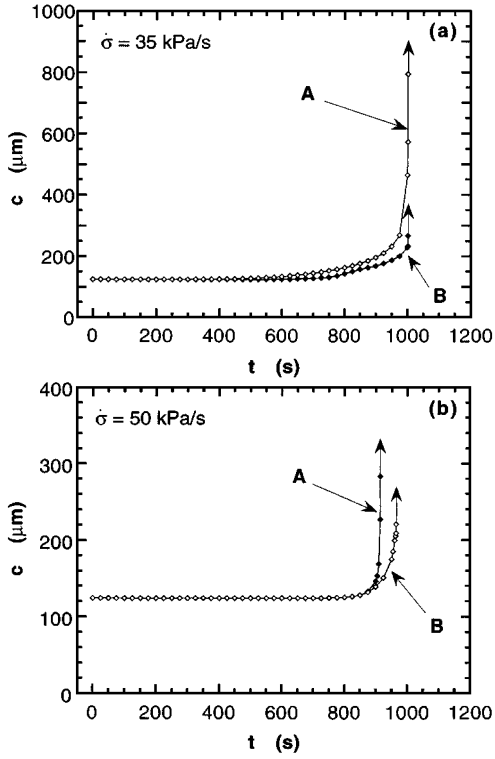

Figure 8 Evolution of the crack size as a function of time for for as-indented (a) and annealed (b) specimens in the dynamic fatigue test. Crack length was evaluated as a function of time by the resolution of Equation 10 under the condition of constant (condition A) and variable (condition B) ψ and χ values. The applied stressing rate is shown.

primarily in the annealed samples, as shown also in Figs 5b and 6b. For as-indented specimens K is a decreasing function of crack size when c is small also in condition A due to the term corresponding to the residual stresses ($K = \chi P/c^{1.5}$). This effect masks the influence of the decreasing value of ψ.

Numerical analysis performed for dynamic fatigue tests furnished different results. Fig. 8 shows the trend of crack length as a function of time. No significant differences can be observed between annealed and as-indented specimens in the two considered conditions. Therefore, the variability of ψ does not noticeably affect the strength in corrosive environment.

The different behaviour observed between static and dynamic fatigue tests for annealed specimens can be explained as follows. In static fatigue the stress is fixed and the crack propagation velocity is ruled by the product $\psi\sqrt{c}$. Therefore, different behaviour is obtained when crack shape factor is constant or variable. When ψ is variable, the crack propagates at very low velocity for $c \approx 200$ μm and this leads to the longer lifetimes. Similar considerations can be applied to the cyclic fatigue tests. Conversely, in dynamic fatigue tests, the applied stress is continuously increased and this compensates for the decrease in ψ. In dynamic test the crack is not free to spend time in a particular position but is driven forward by the increasing stress.

The results shown in Fig. 8 have an important consequence for the use of dynamic fatigue tests in the determination of fatigue parameters. Conventional theory previously presented was developed with the assumption of constant ψ and χ [13, 24]. Results in Fig. 8 demonstrated that Equations 3 and 4 can be used for the calculation of n and v_0 with a high degree of precision. Nevertheless, predictions of lifetime for indented glass specimens subjected to constant or cyclic loads must be calculated taking into account variable ψ and χ values. Analogously, incorrect values can be calculated for n and v_0 from static fatigue tests if conventional indentation fracture mechanics arguments are used without including the variations in ψ and χ.

5. Conclusions

Dynamic, cyclic and static fatigue testing was performed on soda lime silicate glass using indentation strength measurements. In particular, the effect of annealing after the indention process on the fatigue behavior was investigated. Initially, the values of the parameters that describe the fatigue process were obtained from the dynamic fatigue data. For this case, the data from the annealed samples were consistent with those obtained on as-indented specimens. This was not true, however, for the static and cyclic fatigue tests. In this case, the annealed specimens had longer lifetimes than expected theoretically.

In the normal analysis of sub-critical fracture using indentation cracks, the geometric fracture mechanics parameters involved in the analysis are usually considered to be constant. Using previous data in which the crack length dependence of these parameters had been measured, it was possible to obtain consistency between the data from dynamic, cyclic and static fatigue. Using a numerical analysis, the lifetime for materials in the static and cyclic fatigue tests was shown to be sensitive to variations in the stress intensity factor at short crack lengths. It is therefore very important to understand any crack size dependence of the fracture mechanics geometric parameters in this crack size region. For the dynamic fatigue tests, this effect is not so pronounced, as the stress intensity factor is quickly forced to increase in the initial stages of crack propagation.

Acknowledgements

NATO is acknowledged for financial support (CRG 950160).

References

1. S. M. WIEDERHORN, in "Fracture Mechanics of Ceramics," Vol. 2, eds. R. C. Bradt *et al.* (Plenum Press, New York, 1974), pp. 613–46.
2. S. M. WIEDERHORN, in "Fracture Mechanics of Ceramics," Vol. 4, eds. R. C. Bradt *et al.* (Plenum Press, New York, 1978), pp. 549–80.
3. B. R. LAWN, "Fracture of Brittle Solids," 2nd Edition (Cambridge University Press, Cambridge, 1993).
4. J. E. RITTER, JR, in "Fracture Mechanics of Ceramics," Vol. 2, eds. R. C. Bradt et al. (Plenum Press, New York, 1974) pp. 667–86.
5. V. M. SGLAVO and D. J. GREEN, *J. Am. Ceram. Soc.* **78[3]** (1995) 650.
6. P. K. GUPTA and N. J. JUBB, *J. Am. Ceram. Soc.* **64** (1981) C112.
7. D. H. ROACH and A. R. COOPER, *J. Am. Ceram. Soc.* **68[11]** (1985) 632.

8. W. T. HAN, P. HRMA and A. R. COOPER, *Phys. Chem. Glasses*, **30[1]** (1989) 30.
9. S. R. CHOI and J. A. SALEM, *Mat. Sci. Eng.* **A149** (1992) 259.
10. J. SALOMONSON and D. ROWCLIFFE, *J. Am. Ceram. Soc.* **78[1]** (1995) 173.
11. V. M. SGLAVO, L. BRUNDÌ and D. J. GREEN, presented at the 1996 Annual Meeting of the American Ceramic Society, paper n. SXIV-9-96.
12. D. B. MARSHALL and B. R. LAWN, *J. Am. Ceram. Soc.* **63[9–10]** (1980) 532.
13. T. P. DABBS, B. R. LAWN and P. L. KELLY, *Phys. Chem. Glasses* **23[2]** (1982) 58.
14. T. P. DABBS and B. R. LAWN, *Phys. Chem. Glasses* **23[4]** (1982) 121.
15. P. CHANTIKUL, B. R. LAWN, H. RICHTER and S. W. FREIMAN, *J. Am. Ceram. Soc.* **66[7]** (1983) 515.
16. B. L. SYMONDS, R. F. COOK and B. R. LAWN, *J. Mater. Sci.* **18** (1983) 1306.
17. M. YODA, *Engng Fract. Mech.* **28[1]** (1987) 77.
18. G. SORARÙ and R. DAL MASCHIO, *Mater. Sci. Eng.* **85** (1987) L25.
19. T. FETT, D. MUNZ and K. KELLER, *J. Mater. Sci.* **23** (1988) 798.
20. M. YODA and M. NAGAO, *Engng Fract. Mech.* **46[5]** (1993) 789.
21. V. M. SGLAVO and D. J. GREEN, *Acta Metall. Mater*. **43[3]** (1995) 965.
22. P. DWIVEDI and D. J. GREEN, *J. Am. Ceram. Soc.* **78[5]** (1995) 1240.
23. P. DWIVEDI and D. J. GREEN, *J. Am. Ceram. Soc.* **78[8]** (1995) 2122.
24. E. R. FULLER, B. R. LAWN and R. F. COOK, *J. Am. Ceram. Soc.* **66[5]** (1982) 314.
25. B. R. LAWN, D. B. MARSHALL, G. R. ANSTIS and T. P. DABBS, *J. Am. Ceram. Soc.* **66[5]** (1982) 314.
26. S. W. FREIMAN, in "Glass Science and Technology," Vol. 5, eds. D. R. Uhlmann and N. J. Kreidl (Academic Press, London, UK, 1980), pp. 21–78.
27. P. CHANTIKUL, G. R. ANSTIS, B. R. LAWN and D. B. MARSHALL, *J. Am. Ceram. Soc.* **64[9]** (1981) 533.
28. D. B. MARSHALL, B. R. LAWN and P. CHANTIKUL, *J. Mater. Sci.* **14** (1979) 2225.
29. V. M. SGLAVO and D. J. GREEN, *Engng Fract. Mech.* **55[1]** (1996) 35.
30. Y.-W. MAI, X. HU, K. DUAN and B. COTTRELL, in "Fracture Mechanics of Ceramics," Vol. 9, eds. R. C. Bradt *et al*. (Plenum Press, New York, 1992) pp. 387–422.
31. I.-W. CHEN, S.-Y. LIU, D. S. JACOBS and M. ENGINEER, in "Fracture Mechanics of Ceramics," Vol. 12, eds. R. C. Bradt *et al*. (Plenum Press, New York, 1996) pp. 1–13.
32. H. N. HO, in "Fracture Mechanics of Ceramics," Vol. 12, eds. R. C. Bradt *et al*. (Plenum Press, New York, 1996) pp. 15–29.
33. J. CHEVALIER, C. OLAGNON and G. FANTOZZI, in "Fracture Mechanics of Ceramics," Vol. 12, eds. R. C. Bradt *et al*. (Plenum Press, New York, 1978) pp. 45–60.

Received 23 March
and accepted 21 August 1998